Atmospheric
Chemistry
and Physics

Slower ozone production in Houston, Texas following emission reductions: evidence from Texas Air Quality Studies in 2000 and 2006

W. Zhou[1], **D. S. Cohan**[1], **and B. H. Henderson**[2]

[1]Department of Civil and Environmental Engineering, Rice University, Houston, Texas, USA
[2]Environmental Engineering Sciences, University of Florida, Gainesville, Florida, 32611, USA

Correspondence to: D. S. Cohan (cohan@rice.edu)

Abstract. Airborne measurements from two Texas Air Quality Study (TexAQS) field campaigns have been used to investigate changes of ozone production in Houston, Texas, from 2000 to 2006, a period of major emission reduction measures for petrochemical and other sources. Simultaneous declines in nitrogen oxides ($NO_x = NO + NO_2$) and highly reactive volatile organic compounds (HRVOCs) were observed between the two periods. We simulate HO_x (OH and HO_2) and organic radicals with a box model, the Dynamically Simple Model of Atmospheric Chemical Complexity, constrained by available airborne observations. Parameters such as total radical production, total OH reactivity of VOCs and ozone production rate (OPR) are computed to characterize the change of ozone production between 2000 and 2006 in the Houston area. The reduction in HRVOCs led to a decline in total radical production by 20–50 %. Ozone production rates in the Houston area declined by 40–50 % from 2000 to 2006, to which the reduction in NO_x and HRVOCs made large contributions. Despite the significant decline in OPR, ozone production efficiency held steady, and VOC-sensitive conditions dominated during times of most rapid ozone formation, while the slow ozone formation continued to be NO_x-limited. Our results highlight the importance of a balanced approach of ongoing HRVOC controls with NO_x controls to further reduce O_3 levels in the Houston area.
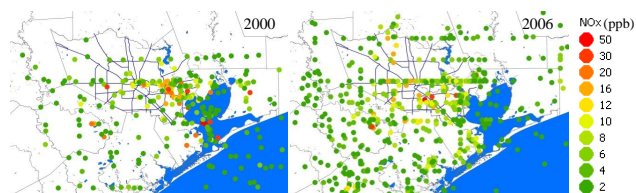
1 Introduction

The Houston metropolitan area has a long history of non-attainment of the US National Ambient Air Quality Standards for ozone (O_3), despite substantial emission reduction efforts since the 1970s (Cowling et al., 2007). Houston ozone events usually occur in spring (April–May) and late summer (August–October) in a bimodal nature. Springtime ozone exceedences tend to occur under post-frontal passage meteorological conditions, while the summertime events often feature continuous high temperature and stagnant meteorology over southeast Texas (Haman et al., 2012; TCEQ, 2007). Favored by these meteorological conditions, large amounts of co-emitted NO_x and VOC from petrochemical facilities in the Houston Ship Channel (HSC) and the nearby urban center lead to high O_3 levels (Fig. 1) (Cowling et al., 2007; Parrish et al., 2009; Ryerson et al., 2003).

Unlike the mobile-dominated hydrocarbon emission compositions in many other metropolitan areas in the US, Houston emissions feature highly reactive VOCs (HRVOC), such as C_2H_4 and C_3H_6, especially in the HSC region (Kim et al., 2011; Ryerson et al., 2003; Washenfelder et al., 2010). HRVOC emissions result from flaring, fugitive emissions, cooling towers, storage/transport, plastics production, and ethylene and propylene production at petrochemical facilities (Kim et al., 2011). Emission inventories for HRVOC are known to be highly uncertain (Kim et al., 2011). Previous studies have concluded that emission inventories in the HSC underestimated HRVOC emissions by at least one order of magnitude (Cowling et al., 2007; Parrish et al., 2009; Ryerson et al., 2003).
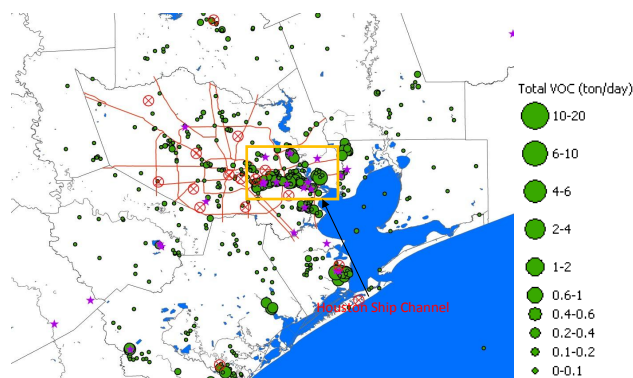
Fig. 1. Map centered on the Houston metropolitan area, showing highways (red lines) and NO_x and VOC point sources. NO_x point sources from a continuous emission monitoring system (CEMS) are shown by purple stars. Green circles indicate total VOC emissions rate (tons day^{-1}) from point sources during TexAQS 2006 (data source: Texas Commission on Environmental Quality). The Houston Ship Channel is identified by a yellow frame. Overall, 17 ground monitors are marked by red-cross-circle.

Fig. 2. The spatial distribution of NO_x concentrations observed by aircraft during TexAQS 2000 and 2006.

The high levels of C_2H_4 and C_3H_6 interacting with NO_x have been shown to foster rapid and efficient O_3 production in Houston (Kleinman et al., 2002a, 2005; Ryerson et al., 2003; Mao et al., 2010). Previous studies have found that OPR in Houston plumes could exceed 100 ppb h^{-1} in contrast to around 20–30 ppb h^{-1} in other metropolitan areas (Kleinman et al., 2002a, 2005).

Despite enormous efforts in curbing HRVOC and NO_x emissions from petrochemical industries and other sources in Houston, peak 8 h O_3 levels have continued to exceed the EPA's 8 h standard (Cowling et al., 2007; Lefer et al., 2010). Meanwhile, up to recently, no study has assessed how the O_3 production and the radical chemistry responded to these emission reductions in the Houston area. Previously, regional transport models were applied to quantify the O_3 trends in the eastern US (Gilliland et al., 2008; Zhou et al., 2013). Using these models to investigate the O_3 trend in the Houston area is hindered by the significant underestimation of historical emissions of some HRVOCs from petrochemical industries and the complexity of local meteorology, such as land–sea breeze and low-level nocturnal jets (Cowling et al., 2007; Parrish et al., 2009).
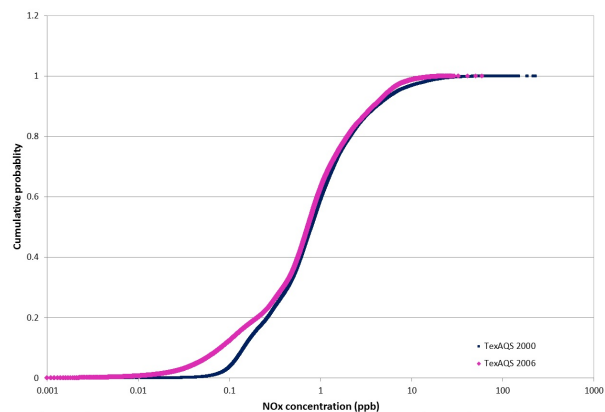
Fig. 3. The cumulative probability distribution of NO_x concentrations in 2000 and 2006 by using 1 s NO_x data from the airborne measurement.

This study averts the shortcomings of the emissions inventories and meteorological simulations by using observation-based analysis and box modeling to explore trends in O_3 production in the Houston area. Aircraft-based measurements of Houston pollution plumes during the Texas Air Quality Studies (TexAQS) in 2000 and 2006 provide a comprehensive data source of air pollutant observations over a time gap of 6 years, during which major emission controls occurred in Houston (Cowling et al., 2007; Parrish et al., 2009; Ryerson et al., 2003). An observation-constrained box model coupled with a subset of the Master Chemical Mechanism (Jenkin et al., 2003; Saunders et al., 2003) is applied to compute HO_x and RO_x radical concentrations for TexAQS 2000 and 2006.

The second section gives a detailed description of the two TexAQS, the airborne measurement techniques and the metrics of ozone production used in this paper. The third section discusses the changes of measured concentrations, analyzes the changes of the ozone production, and explores the O_3 sensitivity to NO_x and VOC. Finally, we discuss the changes of the ozone production through radical budget analysis, the contributions of NO_x and VOC to ozone production and how the O_3 sensitivity to NO_x and VOC changes due to the emission controls of both species.

2 Methodology

2.1 Texas Air Quality Studies (TexAQS) 2000 and 2006

The Texas Air Quality Studies in 2000 and 2006 were designed to investigate sources and atmospheric processes responsible for the formation and transport of photochemical ozone in eastern Texas and the Houston metropolitan area (Figs. 2 and 3) (Cowling et al., 2007; Parrish et al., 2009). The campaigns were conducted from August to September 2000, and September to October 2006. The rapid O_3 formation and abundant emissions of HRVOC were identified
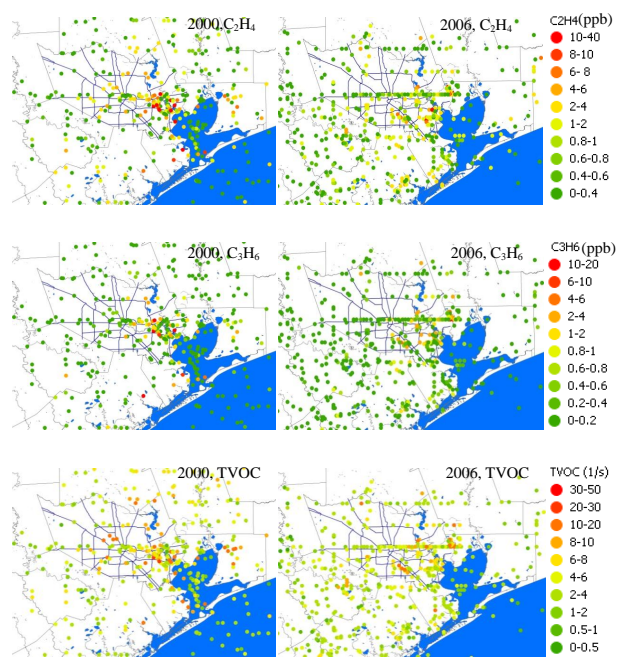
Fig. 4. Spatial distribution of C_2H_4 (top), C_3H_6 (middle), and total VOC reactivity (TVOC) (bottom) in 2000 and 2006.
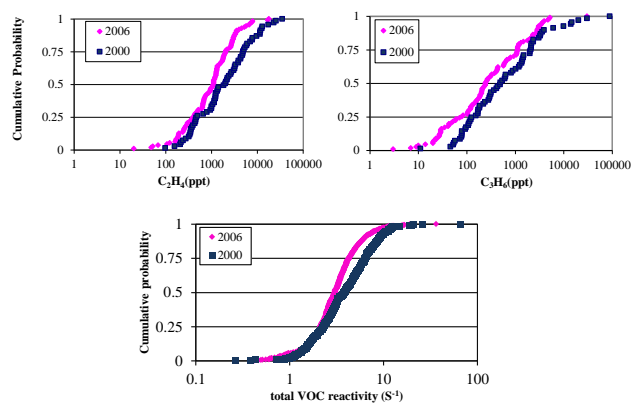
Fig. 5. The cumulative probability distribution of C_2H_4 (top left), C_3H_6 (top right), and total VOC reactivity (bottom) in 2000 and 2006.

in the plumes from petrochemical facilities during TexAQS 2000 (Figs. 4 and 5) (Daum et al., 2004; Kleinman et al., 2002a; Ryerson et al., 2003).

During TexAQS 2000 and 2006, a full spectrum of chemical species was measured by analytical instruments onboard aircraft. During the two studies, the instruments from NOAA onboard the NCAR aircraft (Electra) in 2000 and the NOAA aircraft (WP-3) in 2006 were applied to measure chemical species over the Houston area for 10 days (20, 23, 25, 27, 28, 30 August and 1, 6, 7, and 10 September) in 2000 and for 11 days (13, 15, 19, 20, 21, 25, 26, and 27 September; 5, 6, and 10 October) in 2006. The Electra and WP-3 flew at

Table 1. Summary of O_3 (ppb) and temperature ($^\circ$C) during the two campaigns and monthly average for August, September, and October in 2000 and 2006, all data were measured at 17 ground monitors in the Houston metropolitan area (http://www.tceq.state.tx.us/airquality/monops/historical_data.html).

	Year	Campaign average	August	September	October
O_3	2000	76	72	63	51
(ppb)	2006	58	52	57	47
Temperature	2000	34	34	31	26
($^\circ$C)	2006	30	33	30	27

heights of 400–700 m above ground in afternoon hours when sampling pollution plumes, which was well below the typical planetary boundary layer in eastern Texas. A more comprehensive description of the two studies can be found in previous observational studies (Cowling et al., 2007; Parrish et al., 2009; Ryerson et al., 2003).

2.2 Airborne measurement

Various instruments onboard the aircraft measured atmospheric compounds with a range of time resolutions. Inorganic species (O_3, H_2O, NO_x, HNO_3, SO_2, CO, and CO_2), photolysis rates of chemical species, and meteorological parameters were measured at 1 s time resolution. In both years, hydrocarbons (e.g., HRVOC, isoprene) and oxygenated VOCs (e.g., HCHO, peroxyacetyl nitrate (PAN)) were measured with different instruments at different time resolutions. C_2–C_{10} alkanes, C_2–C_5 alkenes (including C_2H_4 and C_3H_6), ethyne, and C_2–C_5 aldehydes and ketones were measured via whole air samples (WAS) in canisters. Hydrocarbons in WAS were analyzed in laboratories by gas chromatography mass spectrometry (GCMS) for non-methane hydrocarbons (NMHC) (C $\geq$ 3) and gas chromatography with flame ionization detector (GCFID) for NMHC (C_1–C_5). There were a total of 726 WAS measurements in 2000 and 814 in 2006.

A total of 37 VOC species were measured in 2000 and 2006 (alkene: 12 species; alkane: 12 species; oxygenated species: 13 species). HCHO was measured using tunable diode absorption spectrometry with 1 Hz data. Oxygenated VOCs, such as acetic acid, acetone, acetonitrile, methyl ethyl ketone (MEK), methanol, methyl vinyl ketone (MVK) and methacrolein (MACR) were measured by proton transfer reaction mass spectrometry (PTRMS) every 15 s. PAN was measured by chemical ionization mass spectrometry (CIMS). A full description of all chemical species and the corresponding instruments can be found in Table 1a of Parrish et al. (2009).

Four HRVOC species were identified to be critical in the Houston area due to their high concentration and substantial contribution to the local O_3 formation. They are C_2H_4,
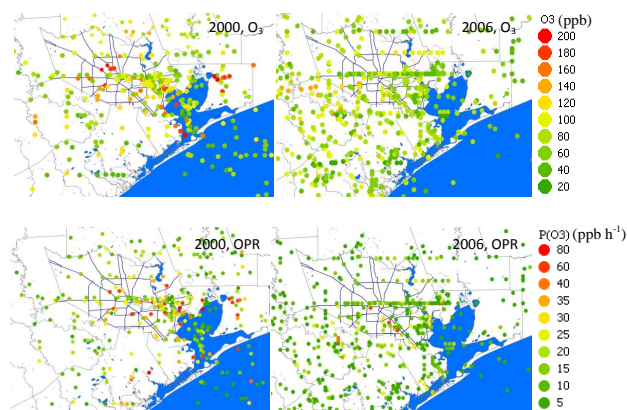
Fig. 6. Spatial distribution of O_3 (top) and OPR (bottom) during TexAQS 2000 and 2006.

C_3H_6, all butene isomers, and 1,3-butadiene. In particular, C_2H_4 and C_3H_6 were the two most important species and were suggested to have the largest impact on ozone production in Houston plumes (Ryerson et al., 2003).

Samples were filtered to remove nighttime samples, since O_3 production occurs only during daytime, and samples that lacked valid measurements of key species (NO, NO_2, O_3, and VOCs). After this processing, there were 472 samples in 2000 and 675 samples in 2006.

Because the airborne samples were essentially discrete, cumulative probability distributions are a good option to compare concentrations between 2000 and 2006. The following analysis will frequently discuss the high (top of 10 % samples, i.e, high OPR means the highest 10 % of samples ranked by OPR), middle (central 20 %), and low (bottom 10 %) samples. For each subset, the mean value of its samples will be compared between 2000 and 2006.

2.3 Observation-based box model

In TexAQS 2000 and 2006, no valid measurements of HO_x and RO_2 were available for computing the ozone production metrics. A box model, the Dynamically Simple Model of Atmospheric Chemical Complexity (DSMACC) (Emmerson and Evans, 2009) based on the kinetic pre-processor (KPP) (Sandu and Sander, 2006), is applied to compute the concentrations of HO_x and RO_2. DSMACC has been applied to simulate radicals in other studies (Henderson et al., 2011, 2012; Stone et al., 2010).

The measured photolysis rates of NO_2, O_3 and HCHO are used to constrain photolysis rates in DSMACC. Meteorological inputs include temperature, pressure, and water mixing ratio. The MCM mechanism used in this study is a subset of the comprehensive MCM v3.2 (http://mcm.leeds.ac.uk/MCM/project.htt#New_3.2) and explicitly represents the 37 VOC species measured in TexAQS 2000 and 2006. It con-

tains 3145 chemical reactions, including 3101 organic reactions and 44 inorganic reactions.

The diurnal steady-state approach (Olson et al., 2012) is applied to constrain the long-lived species to measurement. Each input point of in situ data is integrated by the model to find an internally self-consistent diurnal cycle for all computed species to within a given tolerance (< 0.1 %). Predictions are taken from the computed diurnal cycle at the same time of day as the data for direct comparison of radical predictions and measurements.

2.4 Ozone metrics

In evaluating the ozone production, four commonly used ozone metrics are applied in this study. They are total OH reactivity of VOCs (TVOC), ozone production rate (OPR), the fraction of radicals removed by reactions with NO_x (L_N/Q), and ozone production efficiency (OPE).

The product of the concentration of a VOC species, and its reaction rate with OH, indicates its potential to form first-generation peroxy radicals that facilitate O_3 formation. TVOC is defined in this study as the sum of the OH reactivity of all VOC species and CO (Eq. 1).
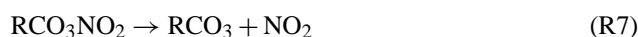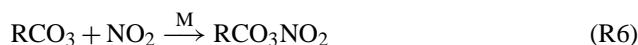
$$\text{TVOC} = k_{\text{CO+OH}}[\text{CO}] + \sum_i k_{\text{VOC}_i+\text{OH}}[\text{VOC}_i] \tag{1}$$

Reactions (R) involved in O_3 formation can be grouped into three categories: radical production (Q), chain propagation, and radical termination (L) (Singh, 1995). Radical production paths generate HO_x and RO_2 radical for chain propagation. The three main radical production reactions are (R1)–(R3) ($Q = 2 \times \text{R1} + 2 \times \text{R2} + \text{R3}$). The radical losses include radical termination by NO_x (R4)–(R7), termed L_N ($= \text{R4} + \text{R5} + \text{R6} - \text{R7}$), and radical–radical combinations to form peroxides (R8)–(R11), termed L_R ($= 2 \times \text{R8} + 2 \times \text{R9} + 2 \times \text{R10} + 2 \times \text{R11}$).

Radical production:

$$O_3 + hv \rightarrow O(^1D) + O_2$$

$$O(^1D) + H_2O \rightarrow 2OH \tag{R1}$$

$$\text{HCHO} + hv \xrightarrow{O_2} 2H_2O + CO \tag{R2}$$

$$\text{Alkene} + O_3 \rightarrow \gamma RO_2 + \cdots \tag{R3}$$

Radical loss via NO_x reactions:

$$OH + NO_2 \xrightarrow{M} HNO_3 \tag{R4}$$

$$RO_2 + NO \rightarrow \text{organic nitrate} \tag{R5}$$

$$RCO_3 + NO_2 \xrightarrow{M} RCO_3NO_2 \tag{R6}$$

$$RCO_3NO_2 \rightarrow RCO_3 + NO_2 \tag{R7}$$

Radical loss via radical–radical combination:

$$HO_2 + HO_2 \rightarrow H_2O_2 + O_2 \tag{R8}$$

$$RO_2 + HO_2 \rightarrow ROOH + O_2 \tag{R9}$$

$$OH + HO_2 \rightarrow H_2O + O_2 \tag{R10}$$

$$RO_2 + R'O_2 \rightarrow RO_2R'O_2 \tag{R11}$$
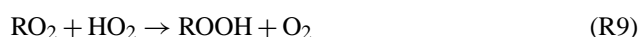
Since NO_2 photolysis is the dominant reaction known to form O_3 in the troposphere, the ozone production rate is equivalent to the formation rate of NO_2 via two production channels: the reaction of HO_2 with NO and the reactions of organic peroxy radical (RO_2) with NO (Eq. 2). NO_2 is also formed by the reaction of NO with O_3, but this cycling of NO_x yields no net change in O_3 during the daytime. The O_3 loss paths ($L(O_3)$) include O_3 photolysis to generate $O(^1D)$ and subsequent formation of OH radical; the reaction of O_3 with OH and HO_2; and the ozonolysis of VOCs (mainly alkenes). Radical loss to aerosol was dominated by HO_2 heterogeneous uptake by aerosols. Radical loss to aerosols is unimportant in the Houston urban area where HO_2 concentration reached ppt levels; in particular, during the two airborne campaign periods in the afternoon hours, aerosol concentration was typically low, and maximal HO_2 was around 50 ppt (Mao et al., 2010). Net_OPR is the difference of OPR and $L(O_3)$ (Eq. 5). FR is the fraction of $O(^1D)$ that generates OH radical rather than returning to ground-state odd oxygen.

$$P(O_3) = k_{HO_2+NO} [HO_2] [NO]$$
$$+ \sum_i k_{RO_2(i)+NO} [RO_2(i)] [NO] \qquad (2)$$

$$L(O_3) = \{ k_{O_3+R} [R] + k_{O_3+HO_2} [HO_2]$$
$$+ k_{O_3+OH} [OH] + FR\, j(O(^1D)) \} [O_3] \qquad (3)$$

$$FR = \frac{k_{O(^1D)+H_2O} [H_2O]}{k_{O(^1D)+H_2O} [H_2O] + k_{O(^1D)+M} [M]} \qquad (4)$$

$$net\_P(O_3) = P(O_3) - L(O_3) \qquad (5)$$

In Eq. (2), k_{HO_2+NO} and $k_{RO_2(i)+NO}$ are the reaction rate coefficients for reactions of HO_2 and RO_2 species with NO. The MCM mechanism in this study has 217 RO_2 species. Since $L(O_3)$ was negligible compared to OPR in polluted daytime samples, we focus our attention on OPR rather than net_OPR.

Whether radicals are removed primarily via reactions with NO_x (L_N) or with other radicals (L_R) depends on the relative abundance of NO_x and radicals. L_N/Q is the fraction of radicals removed via the NO_x reactions, assuming that radical production and removal are in balance (Kleinman, 2005). This metric indicates whether the O_3 formation is NO_x- or VOC-sensitive (Kleinman et al., 1997, 2005). When L_N/Q is less than 0.5, it suggests a low NO_x regime and NO_x-sensitive O_3 formation, while larger values of L_N/Q indicate a high NO_x, VOC-sensitive regime.

Ozone production efficiency (OPE) describes the number of molecules of O_3 generated per molecule of NO_x oxidized into reactive nitrogen species (e.g., HNO_3 and organic nitrate) and can be defined in either of two ways. Accumulative OPE compares aggregate O_3 formation and NO_x loss based on the slope of the least square fit between O_3 and NO_z ($\equiv NO_y$–NO_x, where NO_y is total reactive nitrogen) observations. Accumulative OPE gives an upper limit of actual OPE because NO_z loss via deposition is ignored. Instantaneous

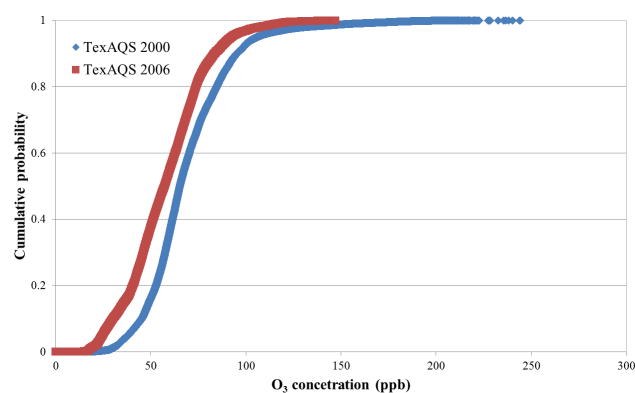**Fig. 7.** The cumulative probability distribution of O_3 in 2000 and 2006 by using 1 s O_3 data from the airborne measurements.

OPE characterizes current rates of O_3 production per NO_x oxidized based on Eq. (6):

$$OPE = P(O_3)/L(NO_x) \qquad (6)$$

$$L(NO_x) = k_{OH+NO_2} [OH] [NO_2]$$
$$+ \sum_i k_{NO+RO_2(i)} [NO] [RO_2(i)]$$
$$+ \sum_i k_{NO_2+RCO_3(i)} [NO_2] [RCO_3(i)]$$
$$- \sum_i k_{RCO_3NO_2(i)} [RCO_3NO_2(i)]. \qquad (7)$$

3 Results

3.1 Changes of NO_x, HRVOC, and O_3 concentration

NO_x and HRVOCs in the Houston area declined by 17 % and 40 %, respectively, between the campaigns, which is consistent with previous studies (Cowling et al., 2007; Gilman et al., 2009; Washenfelder et al., 2010). A more detailed discussion of the change of NO_x and VOC concentrations in the Houston area could be found in Washenfelder (2010). The cumulative distribution of O_3 concentration shows substantial reductions from 2000 to 2006 for high percentile observations, but little change for low percentiles (Fig. 7). This is consistent with Zhou et al. (2013), who found sharper reductions in ozone on peak days than cleaner days in the eastern US.

The daily max 8 h O_3 concentration and daily max temperature averaged over all available ground sites in the Houston area are presented in Figs. S1 and S2. There were a total 17 ground monitors that observed O_3 and temperature in both 2000 and 2006 (Fig. 1). Monthly O_3 concentration in the summer (August, September and October) of 2000 was higher than in 2006 by 4–20 ppb (Table 1). The O_3 level in TexAQS 2000 was higher than in TexAQS 2006 by 18 ppb. Monthly average temperature in summer of 2000 was higher than in 2006 by 1 °C. Temperature during TexAQS 2000 was higher than in TexAQS 2006 by 4 °C. The temperature gap

Table 2. Parameters of O_3 production for the high, middle and low OPR samples for 2000 and 2006*.

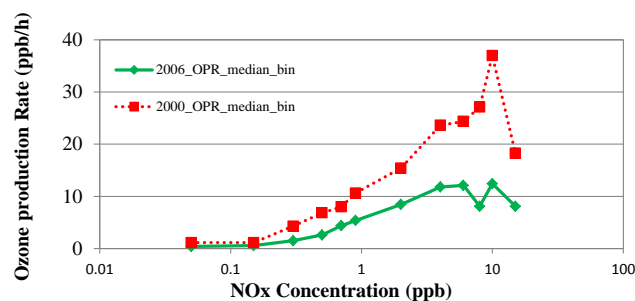| Parameters	High OPR		Middle OPR		Low OPR	
	2000	2006	2000	2006	2000	2006
OPR (ppb h^{-1})	58.9	26.4	12.4	6.4	0.8	0.3
O_3 (ppb)	123	75	80	61	66	57
Q (ppb h^{-1})	12.5	6.1	2.8	2.2	1.1	0.4
NO_x (ppb)	14.1	7.2	4.6	3.2	0.3	1.0
TVOC (s^{-1})	12.0	6.7	4.2	2.8	1.9	1.7
L_N/Q	0.8	0.9	0.5	0.7	0.2	0.2

* All values of parameters are the mean for the subset. The parameters chosen here follow Table 4 of Kleinman et al. (2005). High OPR refers to the top 10 % samples ranked by OPR; middle OPR is the central 20 % samples; and low OPR refers to the bottom 10 % samples.


Fig. 8. OPR as a function of NO_x concentration for 2000 and 2006; measured data is binned by its NO_x concentration and the median values of OPR for each is shown here.

between TexAQS 2000 and TexAQS 2006 was mostly due to extreme hot days from 29 August to 6 September in 2000. Lower O_3 did not entirely result from emissions reductions, as different meteorology, including lower temperatures, also played a role. We acknowledge that changes of O_3 levels from 2000 to 2006 were affected by factors beyond emission changes (Draxler et al., 2000). No method could quantify the contributions of these various factors with observational data. The systemical ozone declines observed over a long period (e.g., 1998–2006) from the TCEQ ground monitors could not be simply explained by the meteorological variations but indicate that emission change played a major role (Cowling et al., 2007).

3.2 Changes of ozone production rate

This section characterizes the decline in ozone production rate (OPR) between the two campaigns and the roles of NO_x and VOC emission reductions in these changes. The spatial distribution of OPR in both years indicates that the hotspots of OPR primarily occurred in the HSC and the closely surrounding areas, and declined in frequency from 2000 to 2006 (Fig. 6). The maximal OPR declined 68 % from 209 ppb h^{-1} in 2000 to 66 ppb h^{-1} in 2006. The maximal OPR in 2000 occurred in the center of the HSC (NO_x: 29 ppb, TVOC: 67 s^{-1}) while the maximal OPR in 2006 (66 ppb h^{-1}) was observed in the eastern portion of the HSC near Mont Belvieu (NO_x: 8 ppb, TVOC: 11 s^{-1}). More broadly, the average of the highest 10 % of OPR declined 55 % from 59 ppb h^{-1} in 2000 to 26 ppb h^{-1} in 2006, while the average of the middle 20 % of OPR declined 48 % from 12 ppb h^{-1} to 6 ppb h^{-1} (Table 2).

The dependence of OPR on NO_x concentration is shown in Fig. 8 for both years. For NO_x concentration < 0.15 ppb, OPR did not show strong response to the change of NO_x concentration for both years. After that, OPR increases rapidly as NO_x increases. OPR tends to increase with NO_x at low NO_x concentration ($NO_x < 10$ ppb). For both years, the peak OPR appears at NO_x near 10 ppb. Beyond this point, OPR declines by 51 % (2000) and 35 % (2006) with further in-

creases in NO_x, because abundant NO_x rapidly removes OH and peroxy radicals. For all NO_x levels, OPR in 2000 was higher than in 2006, showing a downward shift. The downward shift was very clearly visualized in Fig. 8 for NO_x concentration > 0.15 ppb. The median OPR in 2000 was higher in 2006 by 100–200 % for the same NO_x concentration at the NO_x range of 1–15 ppb. The downward shift in the data reflects the role of VOC emission reductions.

The dependence of OPR on TVOC and NO_x concentration in both years is further explored in Fig. 9. There are instances in which high levels of TVOC coincide with high levels of NO_x, indicating collocations of NO_x and VOC emission sources. The high OPR had high levels of NO_x and TVOC with the NO_x / TVOC ratio of around 1 : 1 ppb : 1^{-1} for both years (bottom plots of Fig. 9), similar to the results in Lu et al. (2010) and Kleinman et al. (2005). The differences of the OPR between 2000 and 2006 were (1) more instances of extremely high OPR (> 70 ppb h^{-1}) in 2000, reflecting higher TVOC and NO_x; and (2) for the same levels of NO_x and TVOC ($NO_x < 10$ ppb and TVOC < 10 s^{-1}), OPR in 2000 tended to be higher than in 2006. For the second difference, one of the reasons is that TVOC does not take account of the fast photolysis of much higher aldehyde and ketone levels in 2000 (e.g., HCHO was 13.9 ppb in 2000 and 7.4 ppb in 2006 for the high OPR). Low OPR was associated with the NO_x / TVOC ratio of around 1 : 10.

3.3 Ozone source and radical budget analysis

Although OPR has been reduced, the relative contribution of VOC sources requires further analysis. This section examines the VOC contributions to OPR by examining radical budgets based on the simulations from the DSMACC model. Average OH concentrations simulated by DSMACC were similar in each TaxAQS campaign (1.10×10^7 in 2000 and 1.06×10^7 molecules cm^{-3} in 2006), so OH trends cannot explain the decline of OPR. The contributions of peroxy radicals to OPR at times of rapid O_3 production are summarized in Fig. 10. The HO$_2$–NO reaction contributed about
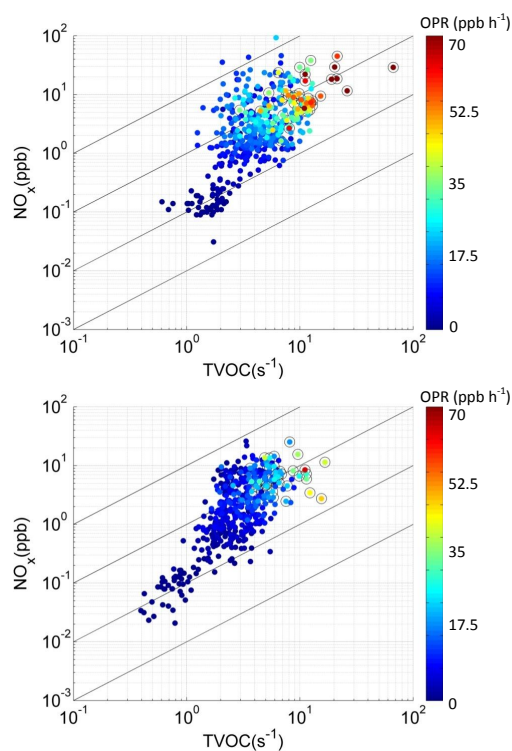
Fig. 9. The dependence of OPR shown in color scale on total VOC reactivity (TVOC) and NO_x concentration for both 2000 and 2006. In the top plots, samples of high OPR are marked by empty circles. Each diagonal line is associated with a constant TVOC to NO_x ratio (from top to bottom, $TVOC / NO_x = 10 : 1, 1 : 1, 1 : 10, 1 : 100$).

60 % of the high OPR in both years, though the rate of this reaction plunged significantly (53 %) from 2000 to 2006.

Among the total 217 RO_2 radicals, 56 species (Table S1 in the Supplement) which contributed more than 95 % of the OPR from the RO_2 and NO reactions are assigned into five groups: $ALKAO_2$, $ALKEO_2$, $CARBO_2$, CH_3O_2, and $ISOPO_2$, approximately reflecting their VOC precursors, i.e., alkanes (C-C), alkenes (C = C), carbonyls, CH_4, and biogenics (Sommariva et al., 2011). Alkenes correspond to HRVOC, while alkanes are mostly anthropogenic saturated hydrocarbons. Carbonyls include a variety of oxygenated VOCs (O-VOCs), such as CH_3CHO, CH_3COCH_3, MEK, and MVK, which may be formed from the OH-oxidation of HRVOCs, isoprene and other long-chain hydrocarbons.

Among the NO and RO_2 reactions, the two largest components were $ALKEO_2$ and $CARBO_2$, the combination of which contributed roughly 25 % of the high OPR in both years. CH_3O_2 contributed only a small amount (8.1 % in 2000 and 11.3 % in 2006) to OPR in this study domain, in contrast to the rural atmosphere, where CH_3O_2 usually contributes about 30 % of OPR (Sommariva et al., 2011). Alkanes and biogenic VOCs had very small contributions to OPR in the two years.
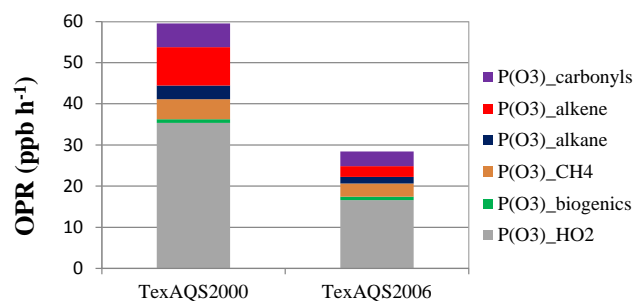
Fig. 10. The contribution of HO_2 and RO_2 radicals to OPR in the high OPR samples (average: 59 ppb h^{-1} in 2000 and 26 ppb h^{-1} in 2006). RO_2 radicals are grouped into five categories based on their VOC precursors.

OPR from RO_2 radicals of alkanes, carbonyls, and HRVOCs declined dramatically from 2000 to 2006: 53 % for $ALKO_2$, 39 % for $CARBO_2$, and 71 % for $ALKEO_2$. Meanwhile, little change was observed from $ISOPO_2$ originating from largely biogenic isoprene, as well as from CH_3O_2 originating from long-lived methane, which has numerous biogenic and anthropogenic sources globally. This is consistent with the decline in anthropogenic VOCs and HRVOC between these periods.

From the OPR source analysis, we have seen that the HO_2 term was the dominant contributor to the high OPR, and its reduction led to the decline of OPR from 2000 to 2006. The HO_2 radical budget for the high OPR samples is examined to investigate sources of HO_2 and how they changed over this period. Total HO_2 production rate declined by 53 % from 3.77×10^8 cm^{-3} s^{-1} in 2000 to 1.75×10^8 cm^{-3} s^{-1} in 2006. Even though HO_2NO_2 formation and decomposition has large weights compared to other HO_2 loss and production processes (Fig. 11), the net of HO_2NO_2 formation and decomposition was only a minor component (3.4–4.5 %) of the HO_2 budget in both years.

Excluding the HO_2NO_2 formation and decomposition, HCHO + OH (18 %), HYPROPO ($OHCH_2C(O\cdot)CH_3$) photolysis (14 %), and HCHO photolysis (13 %) contributed about half of the HO_2 production rate in 2000. In 2006, HCHO + OH (19.1 %), and HCHO photolysis (14.0 %) had similar contributions to the HO_2 production rate, while the contribution of HYPROPO to the HO_2 production rate declined significantly to 8 %.

HYPROPO is predominantly produced from the reaction of C_3H_6 with OH in the MCM. The sources of HCHO in the Houston area have been substantially debated. A few studies using regression analysis of HCHO with primary and secondary pollutants have argued that the primary emission has a larger contribution to ground-level HCHO concentrations than secondary formation (Buzcu Guven and Olaguer, 2011; Olaguer et al., 2009; Rappenglück et al., 2010). However, a comprehensive chemical analysis of airborne HCHO coupled with ground HCHO measurements and emissions data
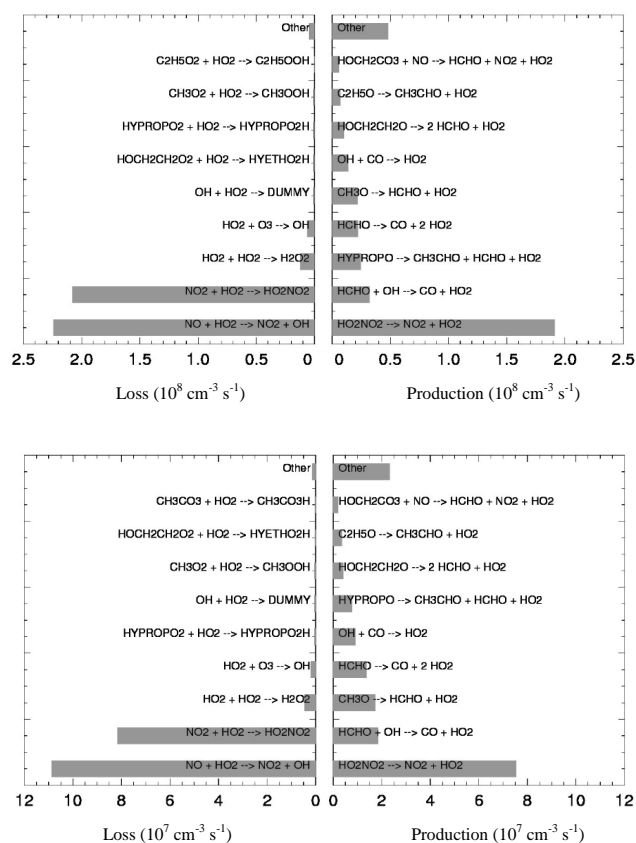
Fig. 11. Loss and production processes of HO_2 radical for high OPR samples. Reactions and species are from the MCM.

concluded that HCHO in HGB was predominantly formed from VOC oxidation (Parrish et al., 2012). We used the same airborne data as Parrish et al. (2009). A careful examination of all airborne data in this study did not find HCHO-only spikes, but observed that the enhancements of HCHO were strongly associated with those of O_3. These two facts are consistent with the claim of Parrish et al. (2012) that HCHO primarily (92 %) resulted from HRVOC oxidation. Median and maximal HCHO declined by 15 % and 21 %, respectively, between the 2000 and 2006 campaigns, with the greatest declines at higher percentiles (Fig. S5). Following this assumption, 40 % of HO_2 production can be attributed to HRVOC as a conservative estimate in both years.

Other minor contributing reactions include the oxidation of $HOCH_2CH_2O$, C_2H_5O, $HOCH_2CO_3$, and IPROPOLO ($OHCH(CH_3)CH_2(O\cdot)$) reactions, contributing a total 15 % of HO_2 production rate. These oxygenated intermediate species and radicals could partially be HRVOC oxidation products. Thus, we conclude that HRVOC played a major role in HO_2 production in both years, and its emission reduction was key to the decline of HO_2 radicals and OPR between the two campaigns.

Aromatics were only minor contributors to the OPR. There were 14 aromatics (benzene, toluene, ethylbenezene, m/p-xylene, o-xylene, styrene, isoproylbenzene, npropylbenzene, 2-ethytoluene, 3-ethytoluene, 4-ethytoluene, 1,3,5-triemthylbenzene, 1,2,4-trimethylbenzene, and 1,2,3-trimethylbenzene) measured by canister during TexAQS 2000 and 2006 (Fig. S6). Among all aromatics, only benzene and toluene contributed 4.5 % of OH reactivity while others' contribution is negligible due to their substantially lower concentrations and small reaction rate constants.

3.4 O_3 sensitivity to NO_x and TVOC

Kleinman (1997) introduced an analytic metric, L_N/Q, to investigate the relative sensitivity of O_3 formation to NO_x and VOC. This formula has been applied to various urban areas (Kleinman et al., 2005; Lu et al., 2010; Mao et al., 2010). When L_N/Q is less than 0.5, it suggests a low NO_x regime and NO_x-sensitive O_3 formation, while larger values of L_N/Q indicate a high NO_x, VOC-sensitive regime. Kleinman (2005) evaluated L_N/Q in five major metropolitan areas (i.e., New York, Philadelphia, Houston, Phoenix, and Nashville). In all five metropolitan areas, high OPR occurred under VOC-sensitive formation ($0.64 < L_N/Q < 0.94$) and median OPR occurred under NO_x-sensitive O_3 formation ($0.12 < L_N/Q < 0.49$). Mao (2010) reported that L_N/Q computed from TRAMP was between 0.2 and 0.4.

In both years, the value of L_N/Q spanned a wide range (0–1), suggesting the airborne data represented a wide variety of O_3 formation chemistry from places in the immediate vicinity of emission sources in HSC to the background atmosphere (Fig. 12). At low NO_x levels (≤ 1 ppb) in both years, low L_N/Q (0–0.5) suggested a NO_x-sensitive O_3 formation. Higher L_N/Q (≥ 0.5) indicated a VOC-sensitive O_3 formation under higher NO_x levels. The L_N/Q distribution over the NO_x-TVOC space presented in this study is similar to the distribution from the G-1 airborne data during TexAQS 2000 (Kleinman et al., 2005). L_N/Q for the high OPR samples (L_N/Q in Table 2) was 0.8 and 0.9, indicating a strongly VOC-sensitive O_3 formation regime for 2000 and 2006, while no significant changes of L_N/Q existed between 2000 and 2006, which reflects the simultaneous declines in NO_x and VOCs.

3.5 Ozone production efficiency

The instantaneous OPE computed from the DSMACC box model considers only the chemical processes and not physical ones such as deposition. As indicated in Eq. (6), instantaneous OPE is OPR divided by $L(NO_x)$. NO_x loss ($L(NO_x)$) is mainly from the reaction of NO_2 with OH (R4) and RCO_3 (R6)–(R7), and the reaction of NO with RO_2 (R5). The average and maximal instantaneous OPEs were 2.0 and 27, consistent with those in other regions (Griffin et al., 2004; Kleinman et al., 2002b).
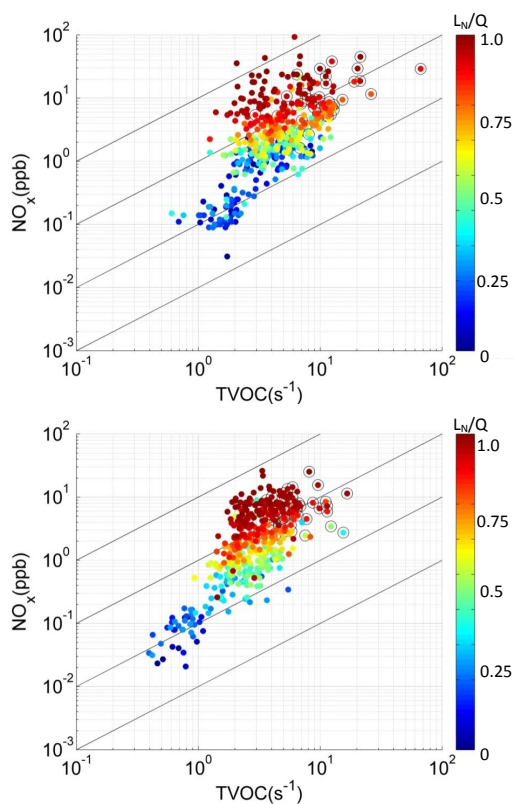
Fig. 12. The dependence of L_N/Q shown in color scale on total VOC reactivity (TVOC) and NO_x concentration for both 2000 and 2006; samples of high OPR are marked by empty circles. Each diagonal line is associated with a constant TVOC to NO_x ratio (from top to bottom, $TVOC/NO_x = 10:1, 1:1, 1:10, 1:100$).

While cloud processing could rapidly remove NO_y in ways not captured by the model and thus lead to overpredictions of OPE (Zhou et al., 2012), MODIS satellite images indicate mostly cloud-free conditions in the immediate vicinity of the transects. Neuman et al. (2009) investigated the correlation between O_3 and NO_x oxidation species from 65 urban and industrial plume transects in the Houston area during TexAQS 2006 and found that OPE was 5.9 ± 1.2 (mean $\pm$ standard deviation), among which the highest OPE (~ 9) was in an isolated petrochemical plume in the Houston Ship Channel. In this work, we found that high OPEs (8–15) were always observed in the diluted industrial plume transects over the isoprene-rich northern rural area, while OPEs in urban and industrial plumes transported southerly tended to be lower (5–7). While both NO_x and VOCs declined significantly by roughly 17–30 %, the accumulative OPEs, derived from the observed O_3 and NO_z of 1 s data samples (e.g., Fig. 13), did not show clear differences between 2000 (5.3 ± 1.1) and 2006 (4.9 ± 1.4). An example was the closely matched OPEs with the highest O_3 between 2000 (5.9–6.7) and 2006 (5.6–6.4) even though both O_3 and NO_z came down substantially (Fig. 13). Specifically, the 1 s data samples of O_3 and NO_z
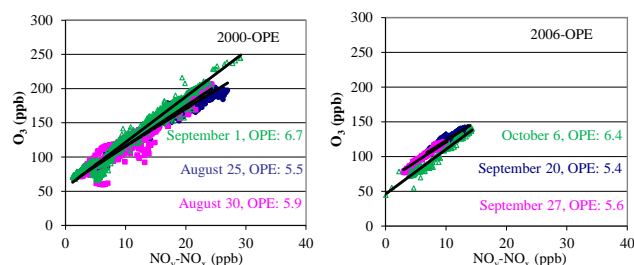
Fig. 13. The accumulative ozone production efficiency (the slope of least square fit between O_3 and NO_z (NO_y–NO_x) concentrations) for the three plumes with the highest O_3 in 2000 (left) and 2006 (right).

species from the plumes transects in which the highest O_3 concentrations were observed were extracted to plot Fig. 13. The instantaneous OPE is not directly comparable to the accumulative OPE because the instantaneous OPE involves only chemical reactions and covers a small temporal and spatial subset of data (Griffin et al., 2004).

4 Discussion and conclusion

Airborne measurements from TexAQS 2000 and 2006 have been used to investigate the change of ozone production in Houston. A box model, DSMACC, has been applied to simulate HO_x and RO_2 radicals with the airborne data. Total radical concentration, OPR, L_N/Q and OPE are compared between 2000 and 2006 at all levels. A comprehensive summary of the comparison of these parameters is presented in Table 2. The parameters shown in Table 2 for 2000 are consistent with the results from the other airborne measurement (118 samples) by the G-1 aircraft during TexAQS 2000 (Kleinman et al., 2005).

Decreased HRVOC emissions are the main cause of reduced radical production (Q in Table 2). Total radicals declined about 51 % and 21 % for the high and middle OPR, reflecting the deeper reductions in the most polluted plumes. HO_2 and RO_2 radicals had similar extents of declines. RO_2 sources were dominated by alkenes (HRVOCs) (30–50 %) and carbonyls (30–40 %). HO_2 radicals were mainly formed from the HCHO reactions and the HRVOC oxidation products. Our analysis linked the radical decline to the decline in HRVOC emissions. More than 40 % of HO_2 production for the high OPR samples could be attributed to HRVOC in both years, and the decline in HRVOCs was critical to the overall decline in radical levels. The simultaneous declines in NO_x and radicals led to a 40–50 % decline in ozone production rate in the Houston area at times of high and middle OPR (Table 2). OPR declined at all levels of NO_x, reflecting the reduction in VOC levels.

The periods of most rapid ozone production were characterized by VOC-sensitive conditions, as indicated by high

levels of L_N/Q in samples with high OPR in both years. Meanwhile, the O_3 sensitivity for the middle OPR shifted from the transition regime ($L_N/Q = 0.5$) to the VOC-sensitive regime ($L_N/Q = 0.7$). OPE remained at similarly high levels (5–15) in both years, due to the similar rates of declines in NO_x and TVOC.

Times of most rapid ozone production in the Houston area were found to be VOC-sensitive (e.g., high OPR in Table 2), and HRVOCs were dominant precursors of peroxy radicals. This suggests the importance of ongoing reductions in HRVOC emissions to achieve further reductions in O_3. Nevertheless, NO_x-sensitive conditions continued to be observed at some times and locations (e.g., low OPR in Table 2) and OPE remained high. This study and others (Kleinman et al., 2005; Xiao et al., 2010; Zhang et al., 2004) indicate a need for a balanced approach to emission reductions for a region characterized by co-existence of NO_x- and VOC-limited formation.

Supplementary material related to this article is available online at http://www.atmos-chem-phys.net/14/2777/2014/acp-14-2777-2014-supplement.pdf.

References

Buzcu Guven, B., and Olaguer, E. P.: Ambient formaldehyde source attribution in Houston during TexAQS II and TRAMP, Atmos. Environ., 45, 4272–4280, 2011.

Cowling, E. B., Furiness, C., Dimitriades, B., Parrish, D., and Estes, M.: Final Rapid Science Synthesis Report: Findings from the Second Texas Air Quality Study (TexAQS II), 2007.

Daum, P. H., Kleinman, L. I., Springston, S. R., Nunnermacker, L. J., Lee, Y. N., Weinstein-Lloyd, J., Zheng, J., and Berkowitz, C. M.: Origin and properties of plumes of high ozone observed during the Texas 2000 Air Quality Study (TexAQS 2000), J. Geophys. Res.-Atmos., 109, D17306, doi:10.1029/2003jd004311, 2004.

Draxler, R.: Meteorological factors of ozone predictability at Houston, Texas, J. Air Waste Manage., 50, 259–271, 2000.

Emmerson, K. M. and Evans, M. J.: Comparison of tropospheric gas-phase chemistry schemes for use within global models, At-

mos. Chem. Phys., 9, 1831–1845, doi:10.5194/acp-9-1831-2009, 2009.

Gilliland, A. B., Hogrefe, C., Pinder, R. W., Godowitch, J. M., Foley, K. L., and Rao, S. T.: Dynamic evaluation of regional air quality models: Assessing changes in O_3 stemming from changes in emissions and meteorology, Atmos. Environ., 42, 5110–5123, 2008.

Gilman, J. B., Kuster, W. C., Goldan, P. D., Herndon, S. C., Zahniser, M. S., Tucker, S. C., Brewer, W. A., Lerner, B. M., Williams, E. J., Harley, R. A., Fehsenfeld, F. C., Warneke, C., and de Gouw, J. A.: Measurements of volatile organic compounds during the 2006 TexAQS/GoMACCS campaign: Industrial influences, regional characteristics, and diurnal dependencies of the OH reactivity, J. Geophys. Res.-Atmos., 114, D00F06, doi:10.1029/2008jd011525, 2009.

Griffin, R. J., Johnson, C. A., Talbot, R. W., Mao, H., Russo, R. S., Zhou, Y., and Sive, B. C.: Quantification of ozone formation metrics at Thompson Farm during the New England Air Quality Study (NEAQS) 2002, J. Geophys. Res.-Atmos., 109, D24302, doi:10.1029/2004jd005344, 2004.

Haman, C. L., Lefer, B., and Morris, G. A.: Seasonal Variability in the Diurnal Evolution of the Boundary Layer in a Near-Coastal Urban Environment, J. Atmos. Ocean. Tech., 29, 697–710, doi:10.1175/jtech-d-11-00114.1, 2012.

Henderson, B. H., Pinder, R. W., Crooks, J., Cohen, R. C., Hutzell, W. T., Sarwar, G., Goliff, W. S., Stockwell, W. R., Fahr, A., Mathur, R., Carlton, A. G., and Vizuete, W.: Evaluation of simulated photochemical partitioning of oxidized nitrogen in the upper troposphere, Atmos. Chem. Phys., 11, 275–291, doi:10.5194/acp-11-275-2011, 2011.

Henderson, B. H., Pinder, R. W., Crooks, J., Cohen, R. C., Carlton, A. G., Pye, H. O. T., and Vizuete, W.: Combining Bayesian methods and aircraft observations to constrain the $HO\bullet + NO_2$ reaction rate, Atmos. Chem. Phys., 12, 653–667, doi:10.5194/acp-12-653-2012, 2012.

Jenkin, M. E., Saunders, S. M., Wagner, V., and Pilling, M. J.: Protocol for the development of the Master Chemical Mechanism, MCM v3 (Part B): tropospheric degradation of aromatic volatile organic compounds, Atmos. Chem. Phys., 3, 181–193, doi:10.5194/acp-3-181-2003, 2003.

Kim, S.-W., McKeen, S. A., Frost, G. J., Lee, S.-H., Trainer, M., Richter, A., Angevine, W. M., Atlas, E., Bianco, L., Boersma, K. F., Brioude, J., Burrows, J. P., de Gouw, J., Fried, A., Gleason, J., Hilboll, A., Mellqvist, J., Peischl, J., Richter, D., Rivera, C., Ryerson, T., te Lintel Hekkert, S., Walega, J., Warneke, C., Weibring, P., and Williams, E.: Evaluations of NO_x and highly reactive VOC emission inventories in Texas and their implications for ozone plume simulations during the Texas Air Quality Study 2006, Atmos. Chem. Phys., 11, 11361-11386, doi:10.5194/acp-11-11361-2011, 2011.

Kleinman, L. I.: The dependence of tropospheric ozone production rate on ozone precursors, Atmos. Environ., 39, 575–586, 2005.

Kleinman, L. I., Daum, P. H., Lee, J. H., Lee, Y., Nan, Nunnermacker, L. J., Springston, S. R., Newman, L., Weinstein, Lloyd, J., and Sillman, S.: Dependence of ozone production on NO and hydrocarbons in the troposphere, Geophys. Res. Lett., 24, 2299–2302, doi:10.1029/97gl02279, 1997.

Kleinman, L. I., Daum, P. H., Imre, D., Lee, Y. N., Nunnermacker, L. J., Springston, S. R., Weinstein-Lloyd, J., and Rudolph, J.:

Ozone production rate and hydrocarbon reactivity in 5 urban areas: A cause of high ozone concentration in Houston, Geophys. Res. Lett., 29, 1467, doi:10.1029/2001gl014569, 2002a.

Kleinman, L. I., Daum, P. H., Lee, Y.-N., Nunnermacker, L. J., Springston, S. R., Weinstein-Lloyd, J., and Rudolph, J.: Ozone production efficiency in an urban area, J. Geophys. Res.-Atmos., 107, 4733, doi:10.1029/2002jd002529, 2002b.

Kleinman, L. I., Daum, P. H., Lee, Y. N., Nunnermacker, L. J., Springston, S. R., Weinstein-Lloyd, J., and Rudolph, J.: A comparative study of ozone production in five U.S. metropolitan areas, J. Geophys. Res.-Atmos., 110, D02301, doi:10.1029/2004jd005096, 2005.

Lefer, B., Rappenglück, B., Flynn, J., and Haman, C.: Photochemical and meteorological relationships during the Texas-II Radical and Aerosol Measurement Project (TRAMP), Atmos. Environ., 44, 4005–4013, 2010.

Lu, K., Zhang, Y., Su, H., Brauers, T., Chou, C., Hofzumahaus, A., Liu, S., Kita, K., Kondo, K., Shao, M., Wahner, A., Wang, J., Wang, X., and Zhu, T.: Oxidant ($O_3 + NO_2$) production processes and formation in regimes in Beijing, J. Geophys. Res.-Atmos., 115, D07303, doi:10.1029/2009JD012714, 2010.

Mao, J., Ren, X., Chen, S., Brune, W. H., Chen, Z., Martinez, M., Harder, H., Lefer, B., Rappenglück, B., Flynn, J., and Leuchner, M.: Atmospheric oxidation capacity in the summer of Houston 2006: Comparison with summer measurements in other metropolitan studies, Atmos. Environ., 44, 4107–4115, 2010.

Neuman, J., Nowak, J., Zheng, W., Flocke, F., Ryerson, T., Trainer, M., Holloway, J., Parrish, D., Frost, G., Peischl, J., Atlas, E., Bahreini, R., Wollny, A., and Fehsenfeld, F.: Relationship between photochemical ozone production and NO_x oxidation in Houston, Texas, J. Geophys. Res.-Atmos., 114, D00F08, doi:10.1029/2008JD011688, 2009.

Olaguer, E. P., Rappenglück, B., Lefer, B., Stutz, J., Dibb, J., Griffin, R., Brune, W. H., Shauck, M., Buhr, M., Jeffries, H., Wiuete, W., and Pinto, J. P.: Deciphering the Role of Radical Precursors during the Second Texas Air Quality Study, J. Air Waste Manage., 59, 1258–1277, doi:10.3155/1047-3289.59.11.1258, 2009.

Olson, J. R., Crawford, J. H., Brune, W., Mao, J., Ren, X., Fried, A., Anderson, B., Apel, E., Beaver, M., Blake, D., Chen, G., Crounse, J., Dibb, J., Diskin, G., Hall, S. R., Huey, L. G., Knapp, D., Richter, D., Riemer, D., Clair, J. St., Ullmann, K., Walega, J., Weibring, P., Weinheimer, A., Wennberg, P., and Wisthaler, A.: An analysis of fast photochemistry over high northern latitudes during spring and summer using in-situ observations from ARCTAS and TOPSE, Atmos. Chem. Phys., 12, 6799–6825, doi:10.5194/acp-12-6799-2012, 2012.

Parrish, D. D., Allen, D. T., Bates, T. S., Estes, M., Fehsenfeld, F. C., Feingold, G., Ferrare, R., Hardesty, R. M., Meagher, J. F., Nielsen-Gammon, J. W., Pierce, R. B., Ryerson, T. B., Seinfeld, J. H., and Williams, E. J.: Overview of the Second Texas Air Quality Study (TexAQS II) and the Gulf of Mexico Atmospheric Composition and Climate Study (GoMACCS), J. Geophys. Res.-Atmos., 114, D00F13, doi:10.1029/2009jd011842, 2009.

Parrish, D. D., Ryerson, T. B., Mellqvist, J., Johansson, J., Fried, A., Richter, D., Walega, J. G., Washenfelder, R. A., de Gouw, J. A., Peischl, J., Aikin, K. C., McKeen, S. A., Frost, G. J., Fehsenfeld, F. C., and Herndon, S. C.: Primary and secondary sources of formaldehyde in urban atmospheres: Houston Texas region,

Atmos. Chem. Phys., 12, 3273–3288, doi:10.5194/acp-12-3273-2012, 2012.

Rappenglück, B., Dasgupta, P. K., Leuchner, M., Li, Q., and Luke, W.: Formaldehyde and its relation to CO, PAN, and SO_2 in the Houston-Galveston airshed, Atmos. Chem. Phys., 10, 2413–2424, doi:10.5194/acp-10-2413-2010, 2010.

Ryerson, T. B., Trainer, M., Angevine, W. M., Brock, C. A., Dissly, R. W., Fehsenfeld, F. C., Frost, G. J., Goldan, P. D., Holloway, J. S., Hübler, G., Jakoubek, R. O., Kuster, W. C., Neuman, J. A., Nicks, D. K., Jr., Parrish, D. D., Roberts, J. M., Sueper, D. T., Atlas, E. L., Donnelly, S. G., Flocke, F., Fried, A., Potter, W. T., Schauffler, S., Stroud, V., Weinheimer, A. J., Wert, B. P., Wiedinmyer, C., Alvarez, R. J., Banta, R. M., Darby, L. S., and Senff, C. J.: Effect of petrochemical industrial emissions of reactive alkenes and NO_x on tropospheric ozone formation in Houston, Texas, J. Geophys. Res.-Atmos., 108, 4249, doi:10.1029/2002jd003070, 2003.

Sandu, A. and Sander, R.: Technical note: Simulating chemical systems in Fortran90 and Matlab with the Kinetic PreProcessor KPP-2.1, Atmos. Chem. Phys., 6, 187–195, doi:10.5194/acp-6-187-2006, 2006.

Saunders, S. M., Jenkin, M. E., Derwent, R. G., and Pilling, M. J.: Protocol for the development of the Master Chemical Mechanism, MCM v3 (Part A): tropospheric degradation of non-aromatic volatile organic compounds, Atmos. Chem. Phys., 3, 161–180, doi:10.5194/acp-3-161-2003, 2003.

Sommariva, R., Bates, T., Bon, D., Brookes, D., Gouw, J., Gilman, J., Herndon, S., Kuster, W., Lerner, B., Monks, P., Osthoff, H., Parker, A., Roberts, J., Tucker, S., Warneke, C., Williams, E., Zahniser, M., and Brown, S.: Modelled and measured concentrations of peroxy radicals and nitrate radical in the U.S. Gulf Coast region during TexAQS 2006, J. Atmos. Chem., 68, 331–362, doi:10.1007/s10874-012-9224-7, 2011.

Singh, H. B.: Composition, Chemistry, and Climate of the Atmosphere, 1 Edn., Wiley, 1995.

Stone, D., Evans, M. J., Commane, R., Ingham, T., Floquet, C. F. A., McQuaid, J. B., Brookes, D. M., Monks, P. S., Purvis, R., Hamilton, J. F., Hopkins, J., Lee, J., Lewis, A. C., Stewart, D., Murphy, J. G., Mills, G., Oram, D., Reeves, C. E., and Heard, D. E.: HO_x observations over West Africa during AMMA: impact of isoprene and NO_x, Atmos. Chem. Phys., 10, 9415–9429, doi:10.5194/acp-10-9415-2010, 2010.

TCEQ: 2006 TEXAQS/GoMACCS Comprehensive Meteorological Analysis of TexAQS II data, 2007.

Washenfelder, R. A., Trainer, M., Frost, G. J., Ryerson, T. B., Atlas, E. L., de Gouw, J. A., Flocke, F. M., Fried, A., Holloway, J. S., Parrish, D. D., Peischl, J., Richter, D., Schauffler, S. M., Walega, J. G., Warneke, C., Weibring, P., and Zheng, W.: Characterization of NO_x, SO2, ethene, and propene from industrial emission sources in Houston, Texas, J. Geophys. Res.-Atmos., 115, D16311, doi:10.1029/2009jd013645, 2010.

Xiao, X., Cohan, D. S., Byun, D. W., and Ngan, F.: Highly nonlinear ozone formation in the Houston region and implications for emission controls, J. Geophys. Res.-Atmos., 115, D23309, doi:10.1029/2010jd014435, 2010.

Zhou, W., Cohan, D. S., Pinder, R. W., Neuman, J. A., Holloway, J. S., Peischl, J., Ryerson, T. B., Nowak, J. B., Flocke, F., and Zheng, W. G.: Observation and modeling of the evolution of

Texas power plant plumes, Atmos. Chem. Phys., 12, 455–468, doi:10.5194/acp-12-455-2012, 2012.

Zhou, W., Cohan, D. S., and Napelenok, S. L.: Reconciling NO_x emissions reductions and ozone trends in the U.S., 2002–2006, Atmos. Environ., 70, 236–244, 2013.